



## Article

# Biosynthesis of Silver Nanoparticles from *Cymbopogon citratus* Leaf Extract and Evaluation of Their Antimicrobial Properties

S M Rakib-Uz-Zaman <sup>1,2,\*</sup> , Ehsanul Hoque Apu <sup>3,4</sup> , Mohammed Nimere Muntasir <sup>1</sup>, Sadrina Afrin Mowna <sup>1</sup>, Mst Gitika Khanom <sup>5</sup>, Shah Saif Jahan <sup>4,6</sup>, Nahid Akter <sup>7</sup>, M. Azizur R. Khan <sup>8</sup>, Nadia Sultana Shuborna <sup>9</sup>, Shahriar Mohd Shams <sup>10</sup> and Kashmery Khan <sup>1</sup>

<sup>1</sup> Biotechnology Program, Department of Mathematics and Natural Sciences, School of Data and Sciences, BRAC University, Dhaka 1212, Bangladesh; nimereemuntasir@gmail.com (M.N.M.); sadrina2012@gmail.com (S.A.M.); kashmery@bracu.ac.bd (K.K.)

<sup>2</sup> Department of Biological Sciences, University of Delaware, Newark, DE 19716, USA

<sup>3</sup> Department of Biomedical Engineering, Institute of Quantitative Health Science and Engineering, Michigan State University, East Lansing, MI 48824, USA; hoqueapu@msu.edu

<sup>4</sup> Centre for International Public Health & Environmental Research, Bangladesh (CIPHER, B), Dhaka 1207, Bangladesh; saifjahanddc@gmail.com

<sup>5</sup> Department of Biotechnology and Genetic Engineering, Islamic University of Kushtia, Kushtia 7003, Bangladesh; gitika12ge@gmail.com

<sup>6</sup> Strathclyde Institute of Pharmacy and Biomedical Sciences (SIPBS), University of Strathclyde, Glasgow G1 1XQ, UK

<sup>7</sup> Dhaka Medical College Hospital, Dhaka 1212, Bangladesh; nahidcmc@gmail.com

<sup>8</sup> Department of Chemistry, Jashore University of Science and Technology, Jashore 7408, Bangladesh; m.azizurrahman.khan@gmail.com

<sup>9</sup> Department of Oral and Maxillofacial Surgery, Faculty of Dentistry, Mahidol University, Bangkok 73170, Thailand; nadiabd4@gmail.com

<sup>10</sup> Department of Orthodontics, Faculty of Dentistry, Bangabandhu Sheikh Mujib Medical University (BSMMU), Shahbag, Dhaka 1000, Bangladesh; shahriar.shams@live.com

\* Correspondence: rakib.zaman@bracu.ac.bd



**Citation:** Rakib-Uz-Zaman, S.M.; Hoque Apu, E.; Muntasir, M.N.; Mowna, S.A.; Khanom, M.G.; Jahan, S.S.; Akter, N.; R. Khan, M.A.; Shuborna, N.S.; Shams, S.M.; et al. Biosynthesis of Silver Nanoparticles from *Cymbopogon citratus* Leaf Extract and Evaluation of Their Antimicrobial Properties. *Challenges* **2022**, *13*, 18. <https://doi.org/10.3390/challe13010018>

Academic Editor: Susan L. Prescott

Received: 23 January 2022

Accepted: 6 April 2022

Published: 5 May 2022

**Publisher's Note:** MDPI stays neutral with regard to jurisdictional claims in published maps and institutional affiliations.



**Copyright:** © 2022 by the authors. Licensee MDPI, Basel, Switzerland. This article is an open access article distributed under the terms and conditions of the Creative Commons Attribution (CC BY) license (<https://creativecommons.org/licenses/by/4.0/>).

**Abstract:** Background: Silver nanoparticles (AgNPs) are toxic to microorganisms and can potentially kill multidrug-resistant bacteria. Nanoparticles can be synthesized in many ways, such as physical or chemical methods. Recently, it has been found that plant molecules can perform the same reduction reactions necessary for the production of nanoparticles but in a much more efficient way. Results: Here, green chemistry was employed to synthesize AgNPs using leaf extracts of *Cymbopogon citratus*. The effects of different parameters such as temperature, pH, and the volume of plant extract were also tested using their absorbance pattern at different wavelengths. The Surface Plasmon Resonance (SPR) changed with the changes in parameters. Changes in temperature from 20 °C to 60 °C have changed the highest absorbance from 0.972 to 3.893 with an SPR of 470 nm. At higher pH (11.1), the particles become highly unstable and have irregular shapes and sizes. The peak shifts to the right at a lower pH level (3.97), indicating a smaller but unstable compound. We have also investigated the effect of the volume of plant extracts on the reaction time. The sample with the highest amount of plant extract showed the most absorbance with a value of 0.963 at  $\lambda_{max}$ , calculated to be 470 nm. The total formation of the AgNPs was observed visually with a color change from yellow to brownish-black. UV-visible spectroscopy was used to monitor the quantitative formation of AgNPs, showing a signature peak in absorbance between 400 and 500 nm. We have estimated the size of the nanoparticles as 47 nm by comparing the experimental data with the theoretical value using Mieplot. The biosynthesized AgNPs showed enhanced antibacterial activity against several multidrug-resistant bacteria, determined based on the minimal inhibitory concentration and zone of inhibition. Conclusion: The findings of this study indicate that an aqueous extract of *C. citratus* can synthesize AgNPs when silver nitrate is used as a precursor, and AgNPs act as antimicrobial property enhancers, which can be used to treat antibiotic-resistant bacteria. Hence, mass production and green synthesis of AgNPs from *C. citratus* will be able to increase the overall health of the general population. Moreover, it will enormously reduce the costs for drug development and provide

employment options in the remotely located source areas. Finally, our findings will influence further studies in this field to better understand the properties and applications of AgNPs and ultimately contribute to improving planetary health by increasing immunity with high biocompatibility and less drug toxicity.

**Keywords:** silver nanoparticles; plant extracts; antimicrobial activity; green chemistry; optimization of parameters; biosynthesis; Surface Plasmon Resonance; UV–visible spectroscopy; size estimation; *Cymbopogon citratus*

## 1. Background

Particles having a diameter of less than 100 nm are termed nanoparticles. Nanoparticles exhibit novel and improved properties based on specific features such as better size, distribution, and morphology compared to their constituent larger particles of the bulk materials. Due to their small size, nanoparticles have a more excellent surface-to-volume ratio. The specific surface area of silver nanoparticles (AgNPs) is essential for their catalytic activity and other associated features such as antibacterial properties [1,2]. Nanoparticles can be synthesized in several ways, such as physical and various other chemical methods. These methods are expensive and use many different toxic substances, which makes them difficult to scale these methods for mass production. In recent years it has been found that plant molecules can perform the same reduction reactions necessary for the production of nanoparticles but in a much more efficient way. Here, green chemistry was employed to synthesize AgNPs using leaf extracts of *Cymbopogon citratus*.

The synthesis of AgNPs is of much interest to the scientific community because of their wide applications. For almost 2000 years, the medicinal benefits of silver have been recognized. Since the nineteenth century, silver compounds have been employed in several antibacterial applications [3]. Silver ions and silver-based compounds are widely acknowledged as lethal to microbes, including some of the most common bacterial strains [4]. These properties make it ideal for various purposes in the medical sector [4]. Topical lotions and creams containing silver reduce burn infection and sores [5]. Medical equipment and implants made from silver embedded polymers are another prominent application. Furthermore, silver-containing consumer products such as colloidal silver cream and silver-integrated fibers are being utilized in sports and athletic equipment [6]. Due to their enhanced antimicrobial activity and their potential application in treating cancers, many researchers are now focusing on developing an effective way to synthesize AgNPs [7]. These AgNPs are also being successfully used in cancer diagnosis and treatment [8,9].

The exact mechanism responsible for the antimicrobial effect of AgNPs is still not clear. Several theories have been put forward to explain the antimicrobial effect of AgNPs. They can attach to the cell wall of bacteria and penetrate it, which subsequently leads to structural damage in the cell wall and membrane with altered permeability of the cell membrane [10]. The nanoparticles are accumulated on the cell surface by forming ‘pits.’ Additionally, the formation of free radicals by the AgNPs may also be responsible for cell death [11]. Numerous studies suggest that they can form free radicals when in contact with the bacteria and damage the bacterial cell membrane by forming pores that result in cell death [12]. It was also suggested that nanoparticles might produce silver ions [13]. These ions can interact and inactivate the thiol groups of many important enzymes [11]. Moreover, the inactivation of the respiratory enzymes by silver ions can also generate reactive oxygen species, attacking the bacterial cell [14].

There are many physical, chemical, and biological methods depicted in various literature on synthesizing AgNPs. The chemical processes include numerous ways that use toxic substances or are expensive and therefore are the ‘not so favored’ synthesis methods [15]. The physical methods include many pieces of high-end equipment, which are expensive and occupy a considerable amount of space. The synthesis of AgNPs with

a tube furnace possesses several disadvantages as a tube furnace is very large, requires much energy (more than several kilowatts) while increasing the temperature around the source material, and also needs a great deal of time (more than 10 min) to be thermally stable [16]. The chemical methods include many toxic components that are harmful to humans when consumed, and they also require harsh physical and chemical conditions, which can be hazardous to human health. In addition, the toxic residues produced along with the nanoparticles during a chemical reduction process make the AgNPs unusable for any kind of biomedical application [17].

### 1.1. Synthesis of Plant Nanoparticles

There has been a significant interest in developing a new strategy to successfully synthesize AgNPs eliminating the drawbacks of chemical and physical production methods. Considering this, the idea of green chemistry has attained considerable recognition, particularly the concepts that are mainly focused on replacing the use of harmful chemicals. Scientists are also focused on developing methods and technologies to reduce and eliminate the compounds harmful to human health and the environment [18]. Among several biological methods, plant extracts for synthesizing AgNPs have gained immense popularity. Owing to its directness in procedures, ease of monitoring, easy sampling, and lower costs, this plant-based technique can be adopted to replace the regularly utilized chemical techniques to facilitate the widespread production of AgNPs [18]. Plant-based nanoparticles are considered eco-friendly as their production methods can effectively replace chemical reduction processes [19]. The metabolites present in plant extracts may aid in the reduction process [19]. Moreover, plants are readily available, easy to grow, and safe to handle.

Fourier transforms infrared spectroscopy (FTIR) spectroscopy of biosynthesized AgNPs has revealed that the biomolecules present in plant extracts are responsible for synthesizing nanoparticles [20]. Terpenoids are one of the biomolecules involved in this process. Terpenoids are commonly referred to as isoprene, an organic molecule that contains five-carbon isoprene compounds. Some studies have suggested that the *Geranium* leaf extract contains terpenoids which contribute the most to AgNPs biosynthesis [20]. Another major plant metabolite is flavonoids, a polyphenolic compound that consists of 15 carbon atoms and is water-soluble [21]. That is why it is imperative that while synthesizing the nanoparticles from the plant extract, the plant must have a high amount of terpenoids and flavonoids and exhibit some medicinal properties of its own. In addition, genetic variations in environmental and ecological factors have made plants chemically very diverse, which further facilitates their application in synthesizing AgNPs [22].

### 1.2. Selection of Plant Extract

*C. citratus*, also known as lemongrass, belongs to the *Gramineae* family. This herb is very rich in essential oil content. The *Cymbopogon* genus is commonly available in the tropical and subtropical areas of Asia, America, and Africa. People have been using *C. citratus* as an everyday tea, insecticide, insect repellent, and a medicinal supplement to treat anti-inflammatory and analgesic diseases worldwide. Medical application of this herb also includes cures for malaria and stomachache due to its antioxidant properties [23]. This plant species was selected in the current study since it has phytochemicals such as flavonoids, alkaloids, tannins, carbohydrates, steroids, and phytosteroids in relatively high concentrations [24]. Medicinal plants have shown their efficiency in treating infectious diseases, diabetes and cancer due to the presence of flavonoids, terpenoids, alkaloids, and phytosteroids [25]. An aqueous extract prepared from the leaves of *C. citratus* was used as both a bioreductant and capping agent for the green synthesis of AgNPs to study the effect of volume of plant extract, reaction temperature, and reaction pH on the AgNPs stability, synthesis rate, and particle size. The AgNPs were prepared using different volumes of *C. citratus* extract, and the response was conducted under different physiological conditions and checked for quality using UV-Vis spectroscopy. Antibacterial effects of the synthesized nanoparticles were also examined by testing them against selected pathogens

such as enterotoxigenic *Escherichia coli* (ETEC), *Salmonella paratyphi*, *Bacillus cereus*, *Vibrio cholera*, *Shigella flexneri*. However, the potentiality of *C. citratus* derived materials obtained from the forests in Bangladesh has not been studied in detail.

### 1.3. Naturally Derived Materials and Plant Extracts Provide Solutions for Global Challenges

Tissue engineering has significantly developed naturally derived materials that are used for plant-derived and biodegradable products [26,27]. While routing for more options for developing widely available options, researchers have also explored self-healing materials as delivery systems for drugs, biomolecules, and tissue regeneration [27,28]. One of the most prevalent naturally derived materials is polymers. Because of their availability and biocompatibility, the most commonly used polymers are collagen, gelatin, chitosan, alginate, etc. Some contain peptides that are ideal for biomedical research applications for wound healing and drug development studies. They help in cellular adhesion, movement, and normal functioning. Silk is also a newly popular option due to its high availability, bulk processability, and elastic properties [26]. Natural extracellular matrices (ECM) have been used in many tissue engineering applications for drug development research [26]. It has been found that patient-derived cancer tissue matrices provide handy options for more realistic results than animal models, which are highly expensive. Even scientists have explored the potential usage of patient-derived ECM products for anti-cancer drug development [29,30]. These approaches save both time and costs because the patient-derived materials are recycled as natural ECM or cancer-tissue mimicking models for studies. Furthermore, discarding this huge amount of diseased tissue is expensive and often creates biohazard risks to the global environment if not properly followed by the standard protocols, which is difficult to maintain in underdeveloped countries due to a lack of proper funding and infrastructures. Genetically engineered rat, mouse, zebrafish, and patient-derived tumor xenografts in animal models are commonly used in vivo models in cancer research [31]. However, they do not replicate the human clinical cancer condition. The closest match to human cancer can be studied by using non-human primates, such as monkeys and chimpanzees [32]. Experts had been trying to convince the National Institute of Health (NIH) to scale back chimpanzee usage in biomedical research, and the NIH announced in 2013 to significantly reduce these procedures [33,34]. The Food and Drug Administration (FDA) delayed clinical trials due to a lack of reliable non-human primates. Unrealistic data often results in the failure of drug trials. The success rate of drugs entering clinical trials and approved by the FDA is only 5.1% in cancer research [35]. These complexities increase the duration and price of drug development and hospital care and create significant obstructions for medication supplies in lower-income countries where people cannot afford expensive treatment options. Usage of plants such as *Cymbopogon citratus* and green synthesis may bridge the gap of the increased need for healthcare products, time, and expenses to combat the planetary health challenges. The herb is widely available and distributed in Asia, Africa, South, and North America. In low-income and underdeveloped communities, its derived materials can provide pharmacological solutions for many pathological diseases due to amazing advantages such as their anti-microbial, anti-obesity, anti-bacterial, anti-oxidants, anti-diarrheal, and anti-inflammatory properties which could enhance immunity [36].

### 1.4. Objectives of This Study

The primary purpose of this study was to figure out if an aqueous extract of *C. citratus*, from the Chittagong Hill Tracts in Bangladesh, can synthesize AgNPs when silver nitrate was used as a precursor. Furthermore, different parameters were tested to optimize the reaction condition and determine which physical and chemical conditions could provide the best results. Most importantly, since AgNPs are potent antimicrobial agent enhancers, they were tested for their antimicrobial properties and investigated how they act when combined with the same plant extract used as the bioreactor for the reaction process.

## 2. Methods

### 2.1. Collection and Preparation of Plant Extract

The whole plant of *C. citratus* is collected from local nurseries and gardens based in Chittagong Hill Tracts, Bangladesh. Formal identification of the plant was conducted based on its characteristics and available information from the nurseries. They were washed thoroughly with distilled water several times to remove dust and dried under shade. After drying, they were rewashed to remove any unwanted dust particles. Then the leaves were dried at room temperature to remove the water from the surface of the leaves. About 10 g of finely incised dried lemongrass leaves were boiled in 150 mL distilled water at 60 °C for about 10 min. The supernatant was filtered using Whatman filter paper No.1 to remove the particulate matter. A dark greenish-yellow clear solution was obtained and stored at 4–8 °C.

### 2.2. Synthesis of Silver Nanoparticles with Aqueous Extract of *C. citratus*

Two mM solution of silver nitrate was prepared by dissolving 0.017 g of AgNO<sub>3</sub> in 50 mL of distilled water as described in [7]. Six ml extract of lemongrass leaf was mixed with 34 mL of 2 mM AgNO<sub>3</sub> solution. The effect of time was studied at regular intervals of 24, 48, 72, and 96 h in the leaf extract. The development of pH was studied by adding NaOH to the solution and bringing the pH to about 11.1. Similarly, to make the solution more acidic, a few drops of concentrated HCl were added to make the pH of the solution 3.97. The reaction was also carried out at different temperatures, such as 20 °C, 40 °C, and 60 °C. The mixture was stirred nonstop, maintaining the aforementioned conditions for 15 min with a magnetic stirrer. We observed the formation of AgNPs by the aqueous extract of *C. citratus*. The AgNPs were repeatedly centrifuged at 3000 rpm for 10 min. The resulting pellets were air-dried and redispersed in deionized distilled water [37].

### 2.3. Characterization of the Silver Nanoparticles

#### 2.3.1. UV–Visible Spectrometric Analysis

The UV–visible spectra of the synthesized AgNPs were recorded as a function of wavelength using a UV–Vis spectrophotometer (Genesys 10 s UV-Vis Spectrophotometer) operated at a resolution of 1 nm. The reduction of silver was measured periodically at 300–700 nm. A spectrum of AgNPs was plotted with the wavelength on the *x*-axis and absorbance on the *y*-axis [37].

#### 2.3.2. Size Estimation of AgNPs

The surface plasmon resonance (SPR) of AgNPs with high symmetry, presenting as spheres or ellipsoids, was calculated with reasonable accuracy by analytical expressions developed in the Mie theory frame [38]. The size was estimated with the software Mieplot (Version 4.6.13, Philip Laven, [www.philiplaven.com/mieplot.htm](http://www.philiplaven.com/mieplot.htm); accessed on 20 June 2020). The calculations were performed by following the manual collected from online sources [39]. First, the refractive index was selected from the advanced drop-down menu as a sphere, silver if particles present in the medium were spherical in nature. Then again, from the advanced drop-down menu refractive index, the surrounding medium, water, was selected. Several calculations were performed and then compared with our experimental data to determine the particle. The particle size of the best-fit spectrum was the particle size determined by Mie Theory [39].

### 2.4. Antibacterial Assays

#### 2.4.1. Bacterial Strain Collection

The bacterial strains such as *E. coli* (ETEC), *S. paratyphi*, *B. cereus*, *V. cholera*, and *S. flexneri* were collected from BRAC University laboratory stock. A loopful of the desired organism was streaked in standard NA (Nutrient Agar) media. The plates were then incubated at 37 °C for 24 h. Then they were stored for further use.



#### 2.4.2. Agar Well Diffusion Method

A suspension of the organism to be tested is prepared in a saline solution and measured equal to 0.5 McFarland standard ( $\sim 1 \times 10^8$  colony forming units (CFU)/mL). The cultures were swabbed on standard MHA (Mueller Hinton Agar) media with a sterile cotton swab. A well with a diameter of approximately 7 mm is made on a Mueller–Hinton Agar plate with a gel puncture. A measure of 60  $\mu$ L of synthesized particles, plant extract, plant extract combined with nanoparticles, and  $\text{AgNO}_3$  solution was inoculated to the well. Then, the plates were incubated in an incubator at 37 °C for 24 h, and the zones of inhibition were discussed [39].

#### 2.4.3. Minimum Inhibitory Concentration (MIC)

The bacterial cultures were grown in Nutrient Broth and transferred to sterile test tubes. Different concentrations of AgNPs (50, 100, 150, 200, and 250  $\mu$ g/mL) were prepared, and 50  $\mu$ L of each concentration was added to every well. The concentration of the stock AgNPs colloidal suspension was calculated following the method mentioned by Khalil et al., 2021 [40]. The test tubes were incubated at 37 °C for 24 h. After incubation, the growth of the bacterial isolates in the test tubes was observed as turbidity using a spectrophotometer at 600 nm. The lowest concentration with no turbidity was determined and noted as the MIC value [41].

### 3. Results

#### 3.1. Synthesis of Silver Nanoparticles

After adding the plant extract to the silver nitrate solution, the solution started to change color (Figure 1). The solution was pale yellow when the reaction started. After 30 min of continuous stirring, the solution slowly turned darker (Figure 1). After 2 h of reaction time, the solution turned completely dark brown, indicating the presence and formation of AgNPs in the mixture (Figure 1).

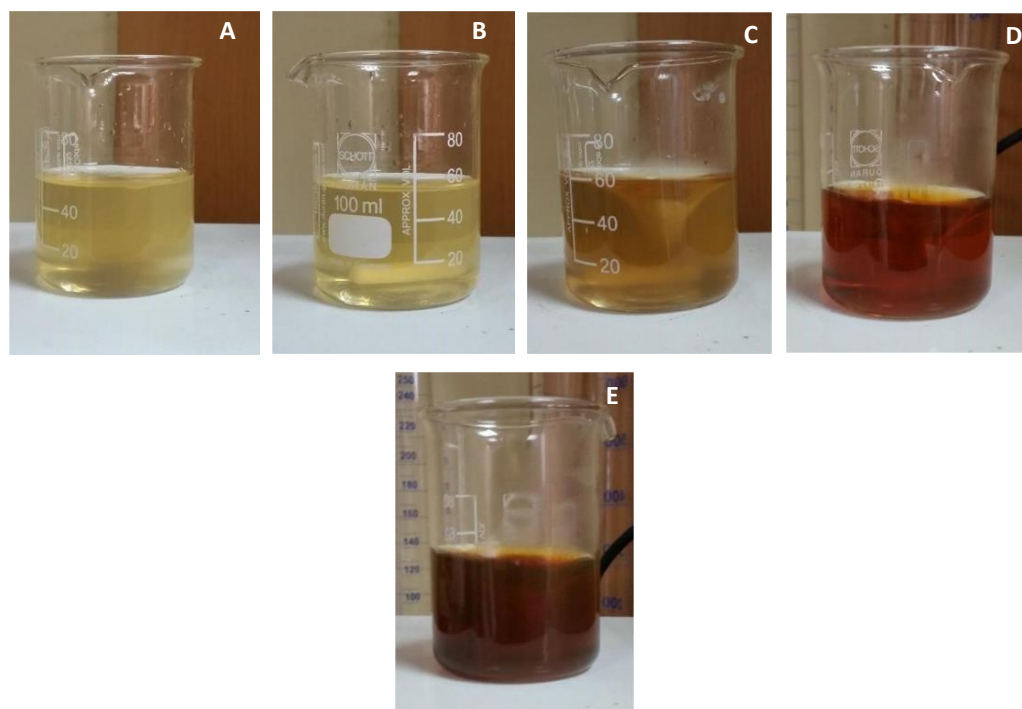


**Figure 1.** Synthesis of AgNPs at different time intervals (A) 15 min, (B) 30 min, (C) 1 h, (D) 1.5 h, and (E) 2 h. (A–E), the colour of the solution turns from a pale yellow to colour to a dark brown colour. The colour is darkest at (E), indicating the presence of AgNPs.

### 3.2. Surface Plasmon Resonance (SPR) Analysis

The AgNPs do not show any absorbance below 390 nm. The highest absorbance was observed at 470 nm, with an absorbance of 2.24 after 24 h of reaction time. This highest peak is the SPR for the synthesized nanoparticles. After 470 nm, the absorbance slowly starts to drop as low as 0.5.

### 3.3. Analyzing the Effect of Temperature

Performing the reaction at different temperatures had a significant impact on the size and shape of the nanoparticles. The SPR changed when the response changed temperature. At 20 °C, the peak was observed at 471 nm, and the highest absorbance after two hours was 0.972. It also had a broader peak compared to the other spectrum. At 60 °C, the peak absorbance was highest at 3.893, with an SPR of 470 nm. The shape of the spectrum was different from the others, with irregular and rigid shapes towards the peak and the peak was also very well defined. The most well-defined peak was observed at 40 °C temperature. While the curve was smooth, the peak was broader than the one with the highest temperature. The SPR was monitored at 469 nm, and the absorbance peaked at 2.237. The wide range of temperature is responsible for the broad peak range of absorbance of AgNPs.

### 3.4. Effect of pH on the Formation of Silver Nanoparticles

The effects of pH on the reaction media can be observed with a visual inspection by looking at the solution. Adding a few drops of concentrated HCl made the solution white. Letting the solution sit for a couple of hours made a white precipitate, which was volatile. The UV spectral analysis revealed that at a pH of (3.97) the peak was observed at 435 nm, which is much lower than the usual SPR of 470 nm. In the case of a higher pH (11.1), the solution quickly turned black with the addition of NaOH. The UV spectrum revealed a random absorbance pattern that did not fit the usual spectral pattern observed in nanoparticle synthesis.

### 3.5. Effect of Plant Extract Volume

The volume of the plant extract had a significant effect on the amount of nanoparticle production. Increasing the volume of the plant extract caused a significant difference in the absorbance pattern. During the 1-h mark, the difference was minimal. As time progressed, during the 3-h mark, the sample with the highest amount of plant extract showed the most absorbance with an absorbance of 0.963 at  $\lambda_{\max}$ , which was calculated to be 470 nm. It was the same with the 4-h mark, with the highest being the same with 12 mL of plant extract and absorbance of 2.031. In contrast, the lowest point was with 8 mL plant extract showing an absorbance of 0.831.

### 3.6. Estimating the Size of the Silver Nanoparticles

Several calculations were made using the Mie Plot tool, using different nanoparticles as our standard model. It has been found that when the particle size is considered to be 47 nm, the spectrum it shows in the theoretical model closely resembles the spectrum created from our experimental values. The theoretical model shows the SPR position at 475 nm, and the experimental model shows the SPR position at 470 nm. So, the size of nanoparticles using lemongrass plant extract can be considered to have a radius of approximately 47 nanometers.

### 3.7. Stability of the Silver Nanoparticles

The nanoparticles were stable for 96 h without adding any sort of extra stabilizers. This is evident by observing the absorbance spectrum at different time intervals. At 24 h, the absorbance peaked at 1.111, with the SPR positioned at 481 nm. Similarly, as time progressed, the absorbance increased. The maximum absorbance was observed at the 96-h mark, showing an absorbance of 1.979. All four curves have a similar pattern with the

SPR at 481 nm. The starting point was also identical in all four of these. Below 390 nm, they showed little to no absorbance. The absorbance increased as time progressed, and the peaks became sharper and well-defined.

### 3.8. Antibacterial Assays

#### 3.8.1. Results of Agar Well Diffusion

The antibacterial assay shows that the largest zone of inhibition was observed for *V. cholerae* in the case of plant extract and nanoparticles, while the lowest zone of inhibition was seen in the case of *B. cereus* (Table 1). Results of the agar well diffusion for nanoparticles showed that the largest zone of inhibition was given by *V. cholerae* while the lowest was achieved by *B. cereus* (Table 1). The zone of inhibition was zero for all pathogens in the plant extract.

**Table 1.** Zone of inhibition of different organisms (all measurements indicated are in mm).

Organism	AgNO <sub>3</sub>	Plant Extract	Nanoparticles	Plant Extract and Nanoparticles
<i>S. paratyphi</i>	11	0	11.5	12
<i>S. flexneri</i>	11	0	12	13
<i>V. cholerae</i>	13	0	13	14
<i>B. cereus</i>	11	0	10	11
<i>E. coli</i> (ETEC)	11.5	0	11.5	12

#### 3.8.2. Results of Minimum Inhibitory Concentration Test

The minimum inhibitory concentration was calculated using the method mentioned earlier. It has been observed that *S. paratyphi* requires the highest concentration of nanoparticles, which is 150 µg/mL. *B. cereus* and *S. flexneri* required the lowest amount of 50 µg/mL of AgNPs.

## 4. Discussion

The attempt to synthesize nanoparticles from aqueous *C. citratus* was successful, as evident from (Figure 1). The color change indicates that nanoparticles began to form in the reaction medium [7]. When a specific plant extract volume was added to the transparent-color AgNO<sub>3</sub> solution, it changed into a pale-yellow color. A while after, the solution was allowed to sit at room temperature, and it slowly began to change color. (Figure 1E) shows that after 2 h of reaction time, the solution became dark brown in color, which is one of the key indications that AgNPs are present in the solution. The gradual color change can be observed in Figure 1A–E, which means that as time went on, the concentration of nanoparticles in the solution was slowly increasing, as evident from the color change from yellow to a much darker tone of brown. After 24 h of reaction time, no more change in color is observed, which means that all the silver molecules in the solution have already been reduced to AgNPs.

Even though the color change can indicate the presence of nanoparticles in the solution, they can only be confirmed by performing UV spectral analysis. Here, we used modern spectrophotometers to correct for the high concentration effect to varying degrees, and therefore it can produce a linear standard curve up to 2.0 Abs units or more. Analyzing the absorbance peak, we can confirm whether AgNPs are present or not. This is because the SPR of the AgNPs determines their optical, physical, and chemical properties. In the case of AgNPs, the absorbance should peak between 400 and 500 nm [7,37]. This peak in absorbance is called their SPR value. Correlating the AgNP's plasmonic properties with their morphology is a fast and easy way to monitor the synthesis by UV–visible spectroscopy [42]. As we can see from Figure 2, the absorbance peaks at 470 nm, which means this is the SPR value of the nanoparticles we were able to synthesize. This peak is more extensive than our reference value [7], which might be because different plants work differently to reduce AgNPs. That is why nanoparticles synthesized using diverse plant samples will have varieties in their shapes and sizes according to the models used as a



bioreactor. Broader peaks indicate larger-sized particles, while smaller particles will form more distinct and well-defined peaks during the UV spectral analysis [38,43].

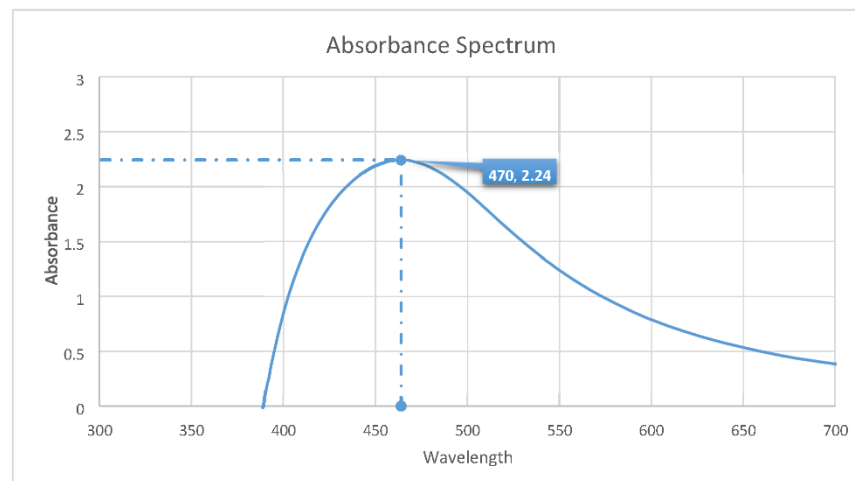


**Figure 2.** Absorbance spectrum of synthesized AgNPs. The highest absorbance was observed at 470 nm, with an absorbance of 2.24. After 470 nm, the absorbance slowly starts to drop, and the lowest absorbance recorded was 0.5 while the absorbance continues to go lower. There is no absorbance observed before an SPR of about 390.

The effect of temperature has an enormous impact on the size and shape of the newly formed AgNPs. We can see clearly from Figure 3 how the spectrum changes concerning the temperature used in the reaction. As the temperature is increased, the peak slowly starts to rise and becomes narrower. At the highest temperature of 60 °C, the peak became more defined, but the spectrum became uneven, and there was much roughness in the spectrum. This was because the increase in temperature caused the nanoparticles to become highly unstable. The noise could also indicate that the solution was not uniform, and particles of various shapes and sizes were available inside the solution. The SPR spectra greatly vary with reaction temperature.

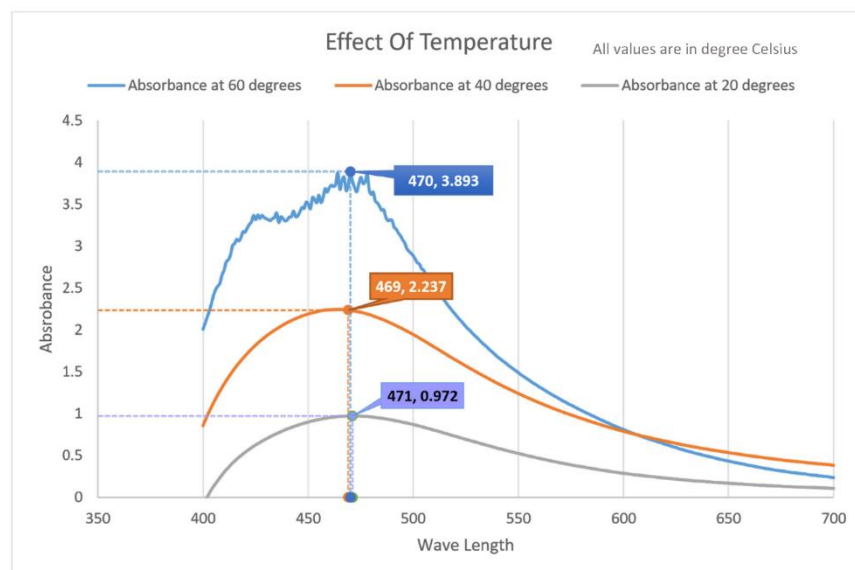


**Figure 3.** Effect of temperature on the size and shape of nanoparticles. At 60 °C, the peak absorbance was recorded highest at 3.893 with an SPR of 470 nm. At 40 °C, the SPR was observed at 469 nm, and the absorbance peaked at 2.237. At 20 °C, the peak was observed at 471 nm, and the highest absorbance was 0.972.

The shape and size distribution of AgNPs is typically measured and visualized using electron microscopy techniques, such as TEM and SEM, or by X-ray diffraction (XRD) studies [44–46]. The SPR band or absorption spectra can be obtained using UV-Visible spectroscopy, where the wavelength corresponding to peak absorbance ( $\lambda_{\text{max}}$ ) reflects the size of the AgNPs. When reaction temperature increases, the absorbance peak increases with an increase in reaction rate, resulting in smaller-sized nanoparticles [20,47]. The temperature enhances the rate of reduction, which results in decreased reaction time. Therefore, a rise in temperature may lead to smaller size AgNPs. The increase in temperature also increases the kinetic energy of molecules, which increases the consumption of silver ions. Thus, particle size growth and formation of uniform-sized AgNPs are less likely [20,48].

The pH of the solution dramatically influences the size, shape, and optical properties of the nanoparticles [49]. At high pH, smaller size AgNPs were obtained compared to low pH values. This difference can be attributed to the difference in the reduction rate of the precursor [49]. As evident from Figure 4, increasing the pH of the medium made the particles highly unstable, and we get a spectrum that indicates that. Lowering the pH to a more acidic medium made the solution completely white instantly. Even though the spectrum is somewhat similar to our usual spectrum, we notice that the peak shifted towards the right side and the size of the nanoparticles became much smaller. The nanoparticles in this medium were highly volatile and could not be separated through repeated centrifugation instead of much heavier and more stable particles at a stable pH of 5.38. This could have happened for various reasons. The change in pH may lead to a change in charge of natural phytochemicals present in an extract. This charge change influenced the adherence of silver ions to biomolecules and might reduce silver ions to AgNPs [50]. Due to the positive charge on silver ions, the negative ionizable groups are attached to silver ions. The reports show that the pH is also a determining factor in the shape, size, production rate, and stability of nanoparticles [20,50].

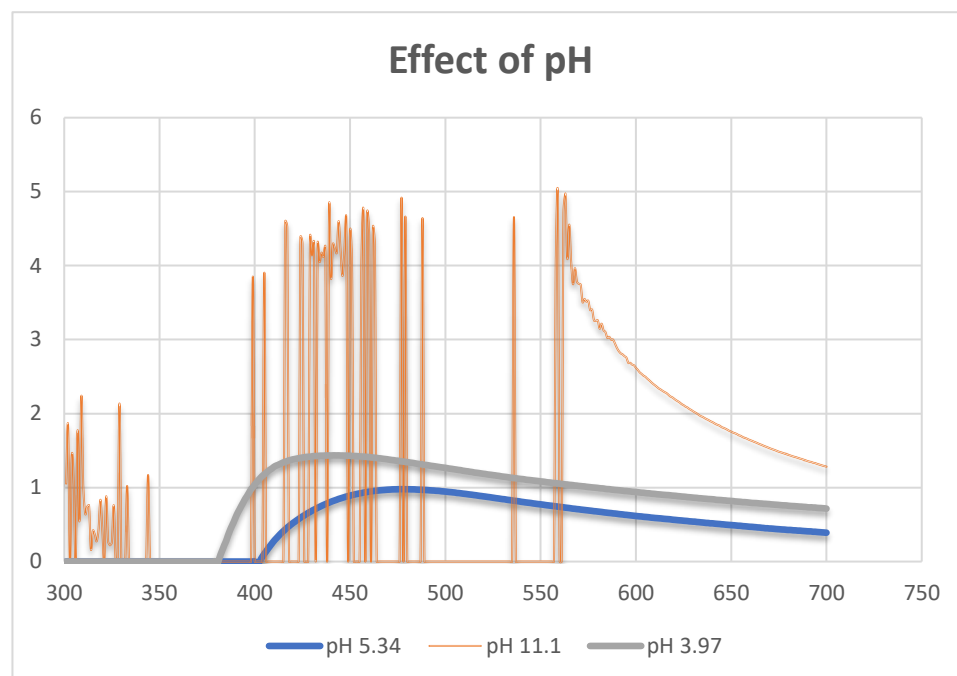


**Figure 4.** Absorbance spectrum of AgNPs at different pH. For a pH of 3.97, the peak was observed at 435 nm. At a pH of 11.1, a random absorbance pattern is observed.

The concentration of plant extracts significantly impacted the reaction time and the concentration of nanoparticles, as we can see from Figure 5. As the amount of plant extract was gradually increased from 8 mL to 12 mL, we could see a significant difference between the reaction medium and the absorbance of the AgNPs. It can be noted that increasing

the volume made the reaction rate high with an increasing concentration of nanoparticles compared to our standard 8 mL of plant extract. This means that the synthesis of AgNPs is greatly affected by the concentration of reducing and stabilizing precursors, which is the plant extract used in the reaction. The increased number of biomolecules results in agglomeration, which reduces the absorption in UV-Vis spectroscopy [20]. As the surface area per mass of a material increases, a more significant amount of the material can come into contact with surrounding materials, thus affecting reactivity. The agglomeration of nanoparticles is due to the adhesion of particles to each other by weak forces leading to (sub) micro-sized entities. In contrast, nanoparticle aggregates are due to the formation of covalent or metallic bonds that cannot be easily disrupted [51]. The particle size and the reaction rate can be controlled by optimizing the amount of plant extract used in the reduction process.

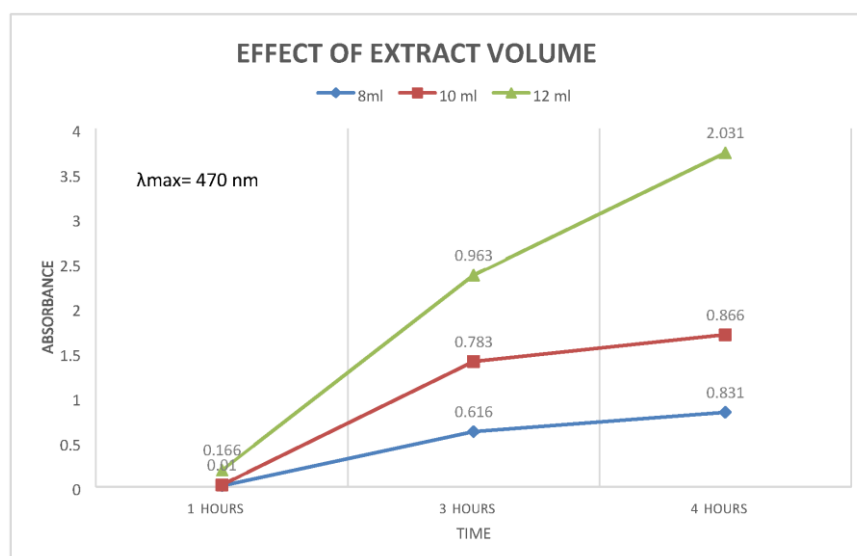


**Figure 5.** Effect of plant extracts volume on the reaction time. At 3 h, the sample containing the highest quantity of plant extract showed the highest absorbance, recorded at 0.963 at  $\lambda_{\max}$  calculated to be 470 nm. The lowest absorbance, 0.616, was shown by the lowest volume of plant extract, 8 mL. At the 4-h mark, the highest was for, once again, the 12 mL of plant extract, showing absorbance of 2.031. The lowest point observed was for the 8 mL plant extract showing absorbance of 0.831.

To determine the particle size in the solutions, we performed several calculations with the computer simulation program Mie Plot v. 4.6.13. It is based on the Mie scattering intensity theory. As one can see, there is only one peak in the absorbance spectra, so we can conclude that our particles are spherical (Figure 6). We can determine the size of particles from the absorbance spectra compared with the calculated one using the Mie theory. The peak position directly depends on the size of nanoparticles; as the size of the particle increases, the SPR position shifts to longer wavelengths. When the particle size is considered 47 nm, the spectrum we get from the theoretical model is the closest match to our experimental values. As we can see from the theoretical model, there is a presence of a secondary peak, which means it has dipole Plasmon resonance, and there are two different sizes of nanoparticles present in the medium. The theoretical spectrum has a higher absorbance than our experimental curve. This could be since we have experimented on a smaller scale. A limited number of particles were present in the medium, hence the lower absorbance value than our reference model. However, these calculations are not exact and cannot confirm that the nanoparticles' size is the actual size we synthesized through the process. Instead, they give us a rough estimate of the AgNPs' size and shape [52]. These calculations have another disadvantage, and that is, they can be applied only to spherical particles. To accurately determine the size and shape of the nanoparticles, FTIR analysis of the AgNPs needs to be performed [7,53].

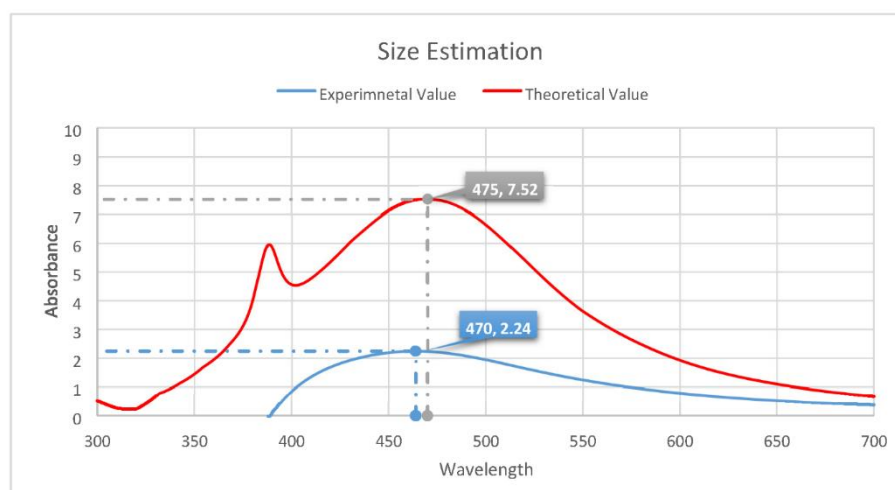


**Figure 6.** Estimating the size of the AgNPs. For the experimental value, the absorbance was revealed to be 2.24 at a wavelength of 470. This is compared with the theoretical value, with an absorbance of 7.52 and a wavelength of 475, to estimate the size of the AgNPs formed.

One of the most crucial aspects of the nanoparticle should be its stability. This means the particles must remain stable either in the suspension or in their solid powder form. If the particles are not stable, it would be impossible to use them for anything as they would be challenging to store under normal conditions. When the nanoparticles are synthesized through physical or chemical means, stabilizers are added to keep them viable for more extended periods. However, plant extract-mediated synthesis of nanoparticles does not require stabilizers as the plant phytochemicals keep them stable and maintain the shape and size of the nanoparticles. In our case, the AgNPs were stable for four days while kept at room temperature (Figure 7). Sunlight can significantly influence the size and shape of the nanoparticles. Sunlight can cause auto-oxidation of the nanoparticles and destabilize them. Usually, these particles are kept away from sunlight and stored in a dark room. In-plant extract mediated synthesis, the sunlight cannot harm the particles as they are surrounded by plant phytochemicals. The curves for each time frame are similar, which means that the shape of the nanoparticles was unchanged through this period (Figure 8). Then again, the SPR values remained constant, meaning that the particles could retain their shape without the addition of stabilizers. However, a zeta potential analysis would provide a more comprehensive view of the stability of the nanoparticles. For molecules and particles that are small enough, a high zeta potential will confer stability, i.e., the solution or dispersion will resist aggregation.

Previous studies proved the strong antibacterial action of AgNPs on either gram-positive or gram-negative bacteria [54,55]. Studies demonstrated that AgNPs could play antimicrobial roles on the multidrug-resistant *P. aeruginosa* in a concentration- and time-dependent manner. The primary mechanism involves the disequilibrium of oxidation and antioxidation processes and the failure to eliminate the excessive ROS [56]. However, to the best of our knowledge, only very few studies reported that AgNPs had antimicrobial activity on multidrug-resistant bacteria. Hence, one of the main objectives of this research project was to check the activity of nanoparticles against different types of multi-drug-resistant pathogenic organisms. In this study, we specifically used multi-drug resistant bacteria for the antimicrobial analysis. The results of the antimicrobial assay have been described in Table 1. The literature review discussed that AgNPs could show enhanced antimicrobial activity when combined with the plant extract. Our results indicate that there is undoubtedly an increase in the combined therapy inhibition zones, but it was not significant enough since the rise is too small. From Table 1, we can see that in the case of *E. coli* (ETEC), the nanoparticles showed an inhibition zone of 11.5 mm, but when combined with plant extract, the inhibition zone slightly increases to 12 mm, which is not much to

say anything for sure. This might be because the antibacterial mechanism of AgNPs may be different from that of antibiotics. However, when we only used plant extract, we have not observed any zone of inhibition because our extract was not purified or because the microbial organisms were multi-drug resistant [57].

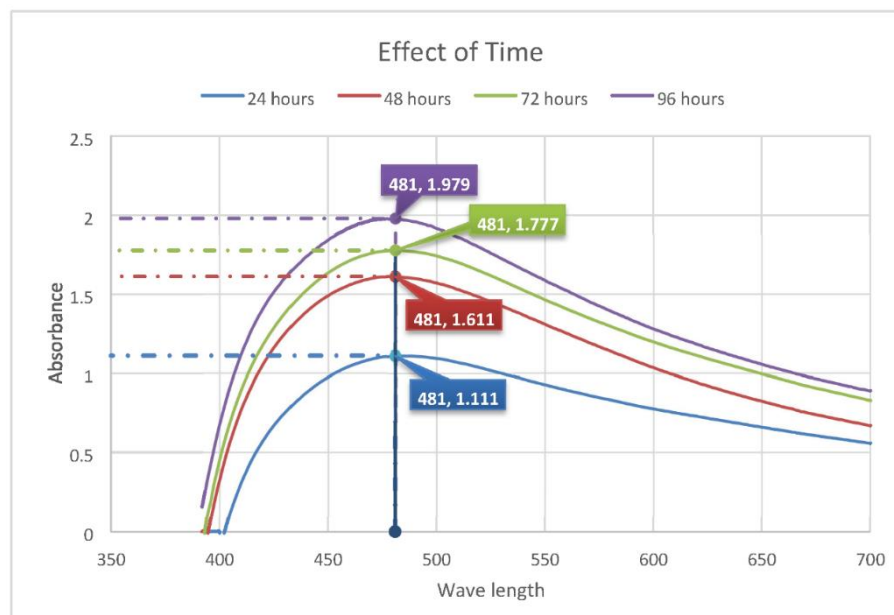


**Figure 7.** Stability of the synthesized AgNPs. The absorbance peaked at 1.111, with the SPR positioned at 481 nm at 24 h. The maximum absorbance was observed at the 96-h mark showing an absorbance of 1.979. At the 48-h mark, the absorbance was 1.611 at an SPR of 481, while at the 72-h mark, the absorbance was 1.777 at an SPR of 481. Little to no absorbance was observed for all of them below 390 nm.

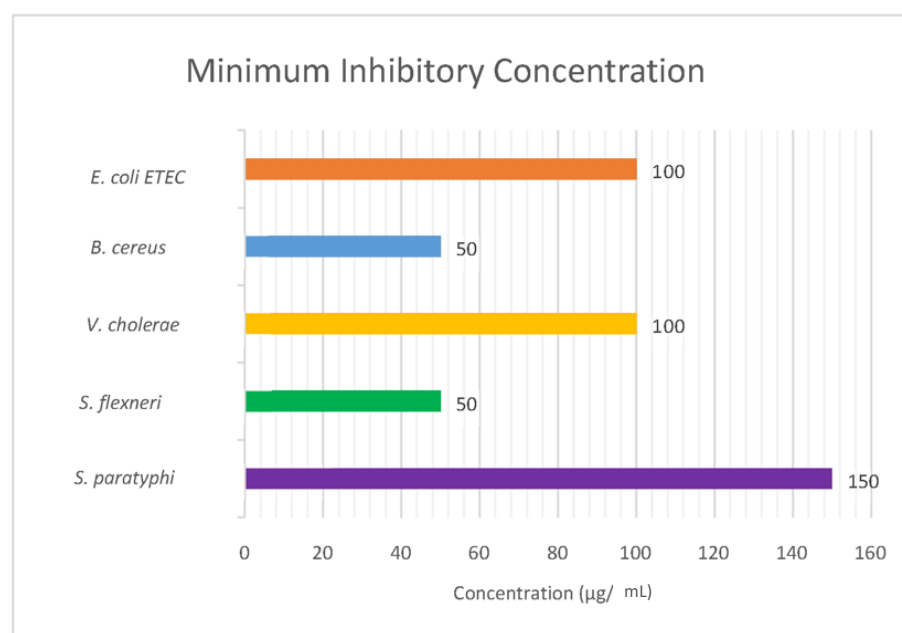


**Figure 8.** Results of the minimum inhibitory test. *S. paratyphi* required the highest concentration of AgNPs at 150 µg/mL, while the lowest amount, 50 µg/mL, was required by *B. cereus* and *S. flexneri*. *E. coli* (ETEC) and *V. Cholerae* required the same concentration of AgNPs at 100 µg/mL.



First, the purification process of the nanoparticles was not performed according to the already established protocol. This was due to the lack of proper equipment while experimenting. As a result, repeated centrifugation was needed, which can sometimes destabilize the particles and significantly hamper their antimicrobial properties. Another important reason could be that the plant extract concentration used in this process was deficient compared to our standard protocol. This was conducted because the plant extract concentration can affect the shape and optical properties of the AgNPs. Optimization is needed in the extract concentration to have a perfect balance between nanoparticle synthesis and its ability to show antimicrobial activity. Increasing the plant extract concentration might yield better results and thus increase the inhibition zones.

Plant-based NPs green synthesis is widely counted as an ideal standard among these green biological techniques owing to its ease of use and the diversity of plants [58]. Greener synthesis of NPs has gained extensive consideration due to their countless benefits, such as non-hazardous, cheaper, and reproducible methods with various applications in clinics, biomedicine, nano-synthesis, and nanotechnologies. It is well known that naturally derived products such as plant-based extracts offer various merits of environment-friendly greener synthesis and biocompatibility for various medicinal and pharmaceutical applications. However, hazardous chemicals are not used for production protocol; therefore, it is ideal and essential for biocompatible therapeutic options [59]. They offer ample opportunities for fighting the global challenges of increased demand for NPs in applications in research and biomedicine [60]. In this study, we have explored and showed the vast plant diversity to be utilized towards rapid and single-step protocol preparatory method with green principles over the conventional ones, promoting environment-friendly natural nanoparticles to overcome global challenges while advancing therapeutic options.

In this manuscript, we highlighted the potentiality of the extract of *C. citratus* for antimicrobial property enhancers, which could be widely used as immunity boosters for the mass population because of availability and lower production cost. Here we have introduced a rare variety of *C. citratus* collected from the wild nature of the Chittagong hill tracts in Bangladesh. Our findings will open up opportunities for future experiments using natural plant extracts. However, one of the shortcomings of this study is that we could not perform the commonly used techniques for characterizing silver NPs, such as UV-vis spectroscopy, X-ray diffractometry (XRD), Fourier transform infrared spectroscopy (FTIR), X-ray photoelectron spectroscopy (XPS), dynamic light scattering (DLS), scanning electron microscopy (SEM), transmission electron microscopy (TEM), and atomic force microscopy (AFM) [61]. Due to the prolonged COVID-19 lockdown in 2020, we could not access the research facilities equipped with the devices mentioned above. Because of the unforeseen global health crisis, we followed the SPR of AgNPs, measured with reasonable accuracy by analytical expressions developed in the Mie theory frame, where size was estimated with the Mieplot software. That is why in this manuscript, we focused on the potential applications of these natural green nanoparticles for biomedical usage rather than characterizing them as ideal nanoparticles. Further studies should be carried out with proper characterization techniques with a considerable amount of in vitro and in vivo model-based biomedical experiments for establishing the Chittagong Hill Tract-based AgNPs for therapeutic applications.

## 5. Conclusions

To conclude, we can say that the objectives set forth before starting this research project have been successful. The primary object was to determine whether the aqueous extract of *C. citratus* can synthesize AgNPs when  $\text{AgNO}_3$  is used as a precursor molecule. The results of the UV spectral analysis clearly show the formation of nanoparticles in the solution. This research was not aimed at using the AgNPs as a substitute for our conventional antibiotics. Rather, it was a steppingstone to show that we can synthesize nanoparticles without using toxic components. Cytotoxic analysis can reveal the adverse effect the nanoparticles have upon consumption by the test, giving us an idea about the dosage requirements without

harming the host cell components. Nanoparticles synthesized through chemical means have tumor-suppressing capabilities. Since our nanoparticles show almost similar optical properties, they can also be tested against cancer cells to see if they can inhibit their growth and potentially kill them. Moreover, the green synthesis of nanoparticles can clean the environment and be used as biosensors to detect contamination. Most importantly, the process used to create the particles does not require any toxic compounds, which is one of the main drawbacks of chemical methods. The field of nanotechnology is growing and still developing. The findings of this research project can influence further studies in this field to understand the technology better and gain more knowledge about the properties and applications of nanoparticles. Nevertheless, green synthesis of these natural biocompatible NPs will ensure environmental conditions and meet the high demand for clinical and biomedical research and drug development. Mass production and green synthesis of the *C. citratus* derived material could increase the overall health of the general population living in densely populated, underdeveloped countries such as Bangladesh. Because of the abundant amount of these leaf extracts, it will enormously reduce the costs for drug development and provide employment options in the remotely located source areas. Ultimately through these steps, these green and naturally derived nanoparticles may contribute to improving planetary health, by increasing immunity with high biocompatibility and less drug toxicity, promoting a green environment for the local environment and our lovely planet.

**Author Contributions:** S.M.R.-U.-Z. and M.N.M. conceived and designed the experiments. M.N.M. performed the experiments; M.N.M., E.H.A., M.G.K., S.S.J., M.A.R.K. and N.S.S. analyzed data and drafted the manuscript; S.M.R.-U.-Z., E.H.A., S.A.M., N.A. and S.M.S. revised the manuscript; K.K., S.M.R.-U.-Z. and E.H.A. wrote the final paper. All authors contributed to revising it critically for important intellectual content. All authors have read and agreed to the published version of the manuscript.

**Funding:** This research received no external funding.

**Institutional Review Board Statement:** Not applicable.

**Informed Consent Statement:** Not applicable.

**Data Availability Statement:** All data generated and analyzed during this study are included in this published article.

**Conflicts of Interest:** The authors declare no conflict of interest.

## References

- Sharma, G.; Jasuja, N.D.; Kumar, M.; Ali, M.I. Biological Synthesis of Silver Nanoparticles by Cell-Free Extract of *Spirulina Platensis*. *J. Nanotechnol.* **2015**, *2015*, 1–6. [\[CrossRef\]](#)
- Ivanova, N.; Gugleva, V.; Dobрева, M.; Pehlivanov, I.; Stefanov, S.; Andonova, V. Silver Nanoparticles as Multi-Functional Drug Delivery Systems. In *Nanomedicines*; Akhyar Farrukh, M., Ed.; IntechOpen: London, UK, 2019; ISBN 978-1-78985-283-7.
- Prabhu, S.; Poulose, E.K. Silver Nanoparticles: Mechanism of Antimicrobial Action, Synthesis, Medical Applications, and Toxicity Effects. *Int. Nano Lett.* **2012**, *2*, 32. [\[CrossRef\]](#)
- Venkataramana, B.; Sankar, S.S.; Kumar, A.S.; Naidu, B.V.K. Synthesis of Silver Nanoparticles Using *Setaria Italica* (Foxtail Millets) Husk and Its Antimicrobial Activity. *Res. J. Nanosci. Nanotechnol.* **2015**, *5*, 6–15. [\[CrossRef\]](#)
- Munteanu, A.; Florescu, I.P.; Nătescu, C. A Modern Method of Treatment: The Role of Silver Dressings in Promoting Healing and Preventing Pathological Scarring in Patients with Burn Wounds. *J. Med. Life* **2016**, *9*, 306–315. [\[PubMed\]](#)
- Sim, W.; Barnard, R.T.; Blaskovich, M.A.T.; Ziora, Z.M. Antimicrobial Silver in Medicinal and Consumer Applications: A Patent Review of the Past Decade (2007–2017). *Antibiotics* **2018**, *7*, e93. [\[CrossRef\]](#)
- Jain, S.; Mehata, M.S. Medicinal Plant Leaf Extract and Pure Flavonoid Mediated Green Synthesis of Silver Nanoparticles and Their Enhanced Antibacterial Property. *Sci. Rep.* **2017**, *7*, 15867. [\[CrossRef\]](#)
- Popescu, M.; Velea, A. Biogenic Production of Nanoparticles. *Dig. J. Nanomater. Biostruct.* **2010**, *6*, 1035–1040.
- Baruwati, B.; Polshettiwar, V.; Varma, R.S. Glutathione Promoted Expeditious Green Synthesis of Silver Nanoparticles in Water Using Microwaves. *Green Chem.* **2009**, *11*, 926. [\[CrossRef\]](#)
- Yin, I.X.; Zhang, J.; Zhao, I.S.; Mei, M.L.; Li, Q.; Chu, C.H. The Antibacterial Mechanism of Silver Nanoparticles and Its Application in Dentistry. *Int. J. Nanomed.* **2020**, *15*, 2555–2562. [\[CrossRef\]](#)
- Mikhailova, E.O. Silver Nanoparticles: Mechanism of Action and Probable Bio-Application. *J. Funct. Biomater.* **2020**, *11*, e84. [\[CrossRef\]](#)

12. Goswami, G.; Boruah, H.; Gautom, T.; Hazarika, D.J.; Barooah, M.; Boro, R.C. Chemically Synthesized Silver Nanoparticles as Cell Lysis Agent for Bacterial Genomic DNA Isolation. *Adv. Nat. Sci. Nanosci. Nanotechnol.* **2017**, *8*, 045015. [\[CrossRef\]](#)
13. Feng, Q.L.; Wu, J.; Chen, G.Q.; Cui, F.Z.; Kim, T.N.; Kim, J.O. A Mechanistic Study of the Antibacterial Effect of Silver Ions on Escherichia Coli and Staphylococcus Aureus. *J. Biomed. Mater. Res.* **2000**, *52*, 662–668. [\[CrossRef\]](#)
14. Xu, H.; Qu, F.; Xu, H.; Lai, W.; Andrew Wang, Y.; Aguilar, Z.P.; Wei, H. Role of Reactive Oxygen Species in the Antibacterial Mechanism of Silver Nanoparticles on Escherichia Coli O157:H7. *Biomaterials* **2012**, *25*, 45–53. [\[CrossRef\]](#) [\[PubMed\]](#)
15. Gudikandula, K.; Charya Maringanti, S. Synthesis of Silver Nanoparticles by Chemical and Biological Methods and Their Antimicrobial Properties. *J. Exp. Nanosci.* **2016**, *11*, 714–721. [\[CrossRef\]](#)
16. Natsuki, J.; Natsuki, T.; Hashimoto, Y. A Review of Silver Nanoparticles: Synthesis Methods, Properties and Applications. *Int. J. Mater. Sci. Appl.* **2015**, *4*, 325. [\[CrossRef\]](#)
17. Ebrahimezhad, A.; Bagheri, M.; Taghizadeh, S.-M.; Berenjian, A.; Ghasemi, Y. Biomimetic Synthesis of Silver Nanoparticles Using Microalgal Secretory Carbohydrates as a Novel Anticancer and Antimicrobial. *Adv. Nat. Sci. Nanosci. Nanotechnol.* **2016**, *7*, 015018. [\[CrossRef\]](#)
18. Shaik, M.; Khan, M.; Kuniyil, M.; Al-Warthan, A.; Alkhathlan, H.; Siddiqui, M.; Shaik, J.; Ahamed, A.; Mahmood, A.; Khan, M.; et al. Plant-Extract-Assisted Green Synthesis of Silver Nanoparticles Using Origanum Vulgare L. Extract and Their Microbicidal Activities. *Sustainability* **2018**, *10*, 913. [\[CrossRef\]](#)
19. Gavade, S.J.M.; Nikam, G.H.; Dhabbe, R.S.; Sabale, S.R.; Tamhankar, B.V.; Mulik, G.N. Green Synthesis of Silver Nanoparticles by Using Carambola Fruit Extract and Their Antibacterial Activity. *Adv. Nat. Sci.* **2015**, *6*, 045015. [\[CrossRef\]](#)
20. Khatoon, N.; Mazumder, J.A.; Sardar, M. Biotechnological Applications of Green Synthesized Silver Nanoparticles. *J. Nanosci. Curr. Res.* **2017**, *2*, 107. [\[CrossRef\]](#)
21. Jain, D.; Daima, H.K.; Kachhwaha, S.; Kothari, S.L. Synthesis of Plant-Mediated Silver Nanoparticles Using Papaya Fruit Extract and Evaluation of their Anti Microbial Activities. *Dig. J. Nanomater. Biostruct.* **2009**, *7*, 557–563.
22. Vokou, D.; Kokkini, S.; Bessiere, J.-M. Geographic Variation of Greek Oregano (Origanum Vulgare Ssp. Hirtum) Essential Oils. *Biochem. Syst. Ecol.* **1993**, *21*, 287–295. [\[CrossRef\]](#)
23. Chukwuocha, U.M.; Fernández-Rivera, O.; Legorreta-Herrera, M. Exploring the Antimalarial Potential of Whole Cymbopogon Citratus Plant Therapy. *J. Ethnopharmacol.* **2016**, *193*, 517–523. [\[CrossRef\]](#) [\[PubMed\]](#)
24. Umar, M.; Mohammed, I.; Oko, J.; Tafinta, I.; Aliko, A.; Jobbi, D. Phytochemical Analysis and Antimicrobial Effect of Lemon Grass (Cymbopogon Citratus) Obtained from Zaria, Kaduna State, Nigeria. *J. Complementary Altern. Med. Res.* **2016**, *1*, 1–8. [\[CrossRef\]](#)
25. Rakib-Uz-Zaman, S.M.; Iqbal, A.; Mowna, S.A.; Khanom, M.G.; Al Amin, M.M.; Khan, K. Ethnobotanical Study and Phytochemical Profiling of Heptapleurum Hypoleucum Leaf Extract and Evaluation of Its Antimicrobial Activities against Diarrhea-Causing Bacteria. *J. Genet. Eng. Biotechnol.* **2020**, *18*, 18. [\[CrossRef\]](#)
26. Ashammakhi, N.; GhavamiNejad, A.; Tutar, R.; Fricker, A.; Roy, I.; Chatzistavrou, X.; Apu, E.H.; Nguyen, K.-L.; Ahsan, T.; Pountos, I.; et al. Highlights on Advancing Frontiers in Tissue Engineering. *Tissue Eng. Part B Rev.* **2021**. [\[CrossRef\]](#) [\[PubMed\]](#)
27. Ashammakhi, N.; Hernandez, A.L.; Unluturk, B.D.; Quintero, S.A.; de Barros, N.R.; Hoque Apu, E.; Bin Shams, A.; Ostrovidov, S.; Li, J.; Contag, C.; et al. Biodegradable Implantable Sensors: Materials Design, Fabrication, and Applications. *Adv. Funct. Mater.* **2021**, *31*, 2104149. [\[CrossRef\]](#)
28. Ashammakhi, N.; Hoque Apu, E.; Caterson, E.J. Self-Healing Biomaterials to Heal Tissues. *J. Craniofacial Surg.* **2021**, *32*, 819–820. [\[CrossRef\]](#) [\[PubMed\]](#)
29. Hoque Apu, E.; Akram, S.U.; Rissanen, J.; Wan, H.; Salo, T. Desmoglein 3–Influence on Oral Carcinoma Cell Migration and Invasion. *Exp. Cell Res.* **2018**, *370*, 353–364. [\[CrossRef\]](#) [\[PubMed\]](#)
30. Salo, T.; Sutinen, M.; Hoque Apu, E.; Sundquist, E.; Cervigne, N.K.; de Oliveira, C.E.; Akram, S.U.; Ohlmeier, S.; Suomi, F.; Eklund, L.; et al. A Novel Human Leiomyoma Tissue Derived Matrix for Cell Culture Studies. *BMC Cancer* **2015**, *15*, 981. [\[CrossRef\]](#) [\[PubMed\]](#)
31. Yee, N.S.; Ignatenko, N.; Finnberg, N.; Lee, N.; Stairs, D. ANIMAL MODELS OF CANCER BIOLOGY. *Cancer Growth Metastasis* **2015**, *8*, 115–118. [\[CrossRef\]](#)
32. Devaux, C.A.; Mediannikov, O.; Medkour, H.; Raoult, D. Infectious Disease Risk Across the Growing Human-Non Human Primate Interface: A Review of the Evidence. *Front. Public Health* **2019**, *7*, 305. [\[CrossRef\]](#) [\[PubMed\]](#)
33. Kaiser, J. Animal Models. Advisers Urge NIH to Scale Back Chimpanzee Research. *Science* **2013**, *339*, 501. [\[CrossRef\]](#) [\[PubMed\]](#)
34. National Institutes of Health (NIH). NIH to Reduce Significantly the Use of Chimpanzees in Research. Available online: <https://www.nih.gov/news-events/news-releases/nih-reduce-significantly-use-chimpanzees-research> (accessed on 31 March 2022).
35. Smietana, K.; Siatkowski, M.; Möller, M. Trends in Clinical Success Rates. *Nat. Rev. Drug Discov.* **2016**, *15*, 379–380. [\[CrossRef\]](#) [\[PubMed\]](#)
36. Oladeji, O.S.; Adelowo, F.E.; Ayodele, D.T.; Odelade, K.A. Phytochemistry and Pharmacological Activities of Cymbopogon Citratus: A Review. *Sci. Afr.* **2019**, *6*, e00137. [\[CrossRef\]](#)
37. Ajayi, E.; Afolayan, A. Green Synthesis, Characterization and Biological Activities of Silver Nanoparticles from Alkalinized Cymbopogon Citratus Stapf. *Adv. Nat. Sci. Nanosci. Nanotechnol.* **2017**, *8*, 015017. [\[CrossRef\]](#)
38. Amendola, V.; Bakr, O.M.; Stellacci, F. A Study of the Surface Plasmon Resonance of Silver Nanoparticles by the Discrete Dipole Approximation Method: Effect of Shape, Size, Structure, and Assembly. *Plasmonics* **2010**, *5*, 85–97. [\[CrossRef\]](#)

39. Muntasir, M.N. Rapid Biological Synthesis of Silver Nanoparticles from Cymbopogon Citratus Extract and Evaluation of Its Antimicrobial Properties. Bachelor's Thesis, BRAC University, Dhaka, Bangladesh, 2018.
40. Khalil, M.A.; El Maghraby, G.M.; Sonbol, F.I.; Allam, N.G.; Ateya, P.S.; Ali, S.S. Enhanced Efficacy of Some Antibiotics in Presence of Silver Nanoparticles Against Multidrug Resistant Pseudomonas Aeruginosa Recovered from Burn Wound Infections. *Front. Microbiol.* **2021**, *12*, 648560. [\[CrossRef\]](#)
41. Ajani, O.O.; Owolabi, T.F.; Olasehinde, G.I.; Akinlabi, D.K.; Owolabi, F.E.; Audu, O.Y. Characterization, Proximate Composition and Evaluation of Antimicrobial Activity of Seed Oil of Bauhinia Tomentosa. *J. Biol. Sci.* **2016**, *16*, 102–111. [\[CrossRef\]](#)
42. Długosz, O.; Banach, M. Continuous Production of Silver Nanoparticles and Process Control. *J. Clust. Sci.* **2019**, *30*, 541–552. [\[CrossRef\]](#)
43. Shankar, S.S.; Rai, A.; Ahmad, A.; Sastry, M. Rapid Synthesis of Au, Ag, and Bimetallic Au Core-Ag Shell Nanoparticles Using Neem (Azadirachta Indica) Leaf Broth. *J. Colloid. Interface. Sci.* **2004**, *275*, 496–502. [\[CrossRef\]](#)
44. Shams, S.; Khan, A.U.; Yuan, Q.; Ahmad, W.; Wei, Y.; Khan, Z.U.H.; Shams, S.; Ahmad, A.; Rahman, A.U.; Ullah, S. Facile and Eco-Benign Synthesis of Au@Fe<sub>2</sub>O<sub>3</sub> Nanocomposite: Efficient Photocatalytic, Antibacterial and Antioxidant Agent. *J. Photochem. Photobiol. B. Biol.* **2019**, *199*, 111632. [\[CrossRef\]](#) [\[PubMed\]](#)
45. Khan, Z.U.H.; Shah, N.S.; Iqbal, J.; Khan, A.U.; Imran, M.; Alshehri, S.M.; Muhammad, N.; Sayed, M.; Ahmad, N.; Kousar, A.; et al. Biomedical and Photocatalytic Applications of Biosynthesized Silver Nanoparticles: Ecotoxicology Study of Brilliant Green Dye and Its Mechanistic Degradation Pathways. *J. Mol. Liq.* **2020**, *319*, 114114. [\[CrossRef\]](#)
46. Ahmad, W.; Khan, A.U.; Shams, S.; Qin, L.; Yuan, Q.; Ahmad, A.; Wei, Y.; Khan, Z.U.H.; Ullah, S.; Rahman, A.U. Eco-Benign Approach to Synthesize Spherical Iron Oxide Nanoparticles: A New Insight in Photocatalytic and Biomedical Applications. *J. Photochem. Photobiol. B. Biol.* **2020**, *205*, 111821. [\[CrossRef\]](#) [\[PubMed\]](#)
47. Ibrahim, H.M.M. Green Synthesis and Characterization of Silver Nanoparticles Using Banana Peel Extract and Their Antimicrobial Activity against Representative Microorganisms. *J. Radiat. Res. Appl. Sci.* **2015**, *8*, 265–275. [\[CrossRef\]](#)
48. Verma, A.; Mehata, M.S. Controllable Synthesis of Silver Nanoparticles Using Neem Leaves and Their Antimicrobial Activity. *J. Radiat. Res. Appl. Sci.* **2016**, *9*, 109–115. [\[CrossRef\]](#)
49. Alqadi, M.K.; Abo Noqtah, O.A.; Alzoubi, F.Y.; Alzoubi, J.; Aljarrah, K. PH Effect on the Aggregation of Silver Nanoparticles Synthesized by Chemical Reduction. *Mater. Sci.-Pol.* **2014**, *32*, 107–111. [\[CrossRef\]](#)
50. Dubey, S.P.; Lahtinen, M.; Sillanpää, M. Tansy Fruit Mediated Greener Synthesis of Silver and Gold Nanoparticles. *Process Biochem.* **2010**, *45*, 1065–1071. [\[CrossRef\]](#)
51. Gosens, I.; Post, J.A.; de la Fonteyne, L.J.; Jansen, E.H.; Geus, J.W.; Cassee, F.R.; de Jong, W.H. Impact of Agglomeration State of Nano- and Submicron Sized Gold Particles on Pulmonary Inflammation. *Part. Fibre Toxicol.* **2010**, *7*, 37. [\[CrossRef\]](#)
52. Šileikaitė, A.; Puiso, J.; Prosycevas, I.; Tamulevičius, S. Investigation of Silver Nanoparticles Formation Kinetics During Reduction of Silver Nitrate with Sodium Citrate. *Medžiagotyra* **2009**, *15*, 21–27.
53. Khan, A.U.; Wei, Y.; Khan, Z.U.H.; Tahir, K.; Khan, S.U.; Ahmad, A.; Khan, F.U.; Cheng, L.; Yuan, Q. Electrochemical and Antioxidant Properties of Biogenic Silver Nanoparticles. *Int. J. Electrochem. Sci.* **2015**, *10*, 12.
54. Sonidi, I.; Salopek-Sonidi, B. Silver Nanoparticles as Antimicrobial Agent: A Case Study on E. Coli as a Model for Gram-Negative Bacteria. *J. Colloid Interface Sci.* **2004**, *275*, 177–182. [\[CrossRef\]](#)
55. Shameli, K.; Ahmad, M.B.; Jazayeri, S.D.; Shabanzadeh, P.; Sangpour, P.; Jahangirian, H.; Gharayebi, Y. Investigation of Antibacterial Properties Silver Nanoparticles Prepared via Green Method. *Chem. Cent. J.* **2012**, *6*, 73. [\[CrossRef\]](#) [\[PubMed\]](#)
56. Liao, S.; Zhang, Y.; Pan, X.; Zhu, F.; Jiang, C.; Liu, Q.; Cheng, Z.; Dai, G.; Wu, G.; Wang, L.; et al. Antibacterial Activity and Mechanism of Silver Nanoparticles against Multidrug-Resistant Pseudomonas Aeruginosa. *Int. J. Nanomed.* **2019**, *14*, 1469–1487. [\[CrossRef\]](#) [\[PubMed\]](#)
57. Gonelimali, F.D.; Lin, J.; Miao, W.; Xuan, J.; Charles, F.; Chen, M.; Hatab, S.R. Antimicrobial Properties and Mechanism of Action of Some Plant Extracts Against Food Pathogens and Spoilage Microorganisms. *Front. Microbiol.* **2018**, *9*, 1639. [\[CrossRef\]](#) [\[PubMed\]](#)
58. Hano, C.; Abbasi, B.H. Plant-Based Green Synthesis of Nanoparticles: Production, Characterization and Applications. *Biomolecules* **2021**, *12*, 31. [\[CrossRef\]](#)
59. Bhardwaj, B.; Singh, P.; Kumar, A.; Kumar, S.; Budhwar, V. Eco-Friendly Greener Synthesis of Nanoparticles. *Adv. Pharm. Bull.* **2020**, *10*, 566–576. [\[CrossRef\]](#)
60. Rendón-Villalobos, R.; Ortiz-Sánchez, A.; Tovar-Sánchez, E.; Flores-Huicochea, E. The Role of Biopolymers in Obtaining Environmentally Friendly Materials. In *Composites from Renewable and Sustainable Materials*; Poletto, M., Ed.; InTech: London, UK, 2016; ISBN 978-953-51-2793-2.
61. Zhang, X.-F.; Liu, Z.-G.; Shen, W.; Gurunathan, S. Silver Nanoparticles: Synthesis, Characterization, Properties, Applications, and Therapeutic Approaches. *Int. J. Mol. Sci.* **2016**, *17*, E1534. [\[CrossRef\]](#)